Calibration of Smart Antennas in a GSM Network

Karlheinz Pensel[1], Hicham Aroudaki[2], and Josef A. Nossek[1]

[1] Institute for Network Theory and Circuit Design
Munich University of Technology
D-80290 Munich, Germany
e-mail: kape@nws.e-technik.tu-muenchen.de
Phone/Fax: +49 (89) 289-28509 / -28504

[2] Mannesmann Mobilfunk GmbH
Am Seestern 1
D-40543 Düsseldorf, Germany
hicham.aroudaki@d2privat.de
+49 (211) 533-3422 / -2124

Keywords: calibration, GSM network, signal processing, antenna array

Abstract

Smart antennas can achieve a considerable gain in spectral efficiency provided that errors due to mutual coupling and amplitude or phase errors of the antenna elements are negligible. Calibration by the knowledge of directions of wavefronts transmitted by a second base station lessens the influence of these imperfections. This study describes the calibration results of general planar antenna arrays in the existing GSM network of the German network operator Mannesmann Mobilfunk GmbH. The presented direction based calibration algorithm does not only take multipath propagation of discrete wavefronts but also a considerable angular spread into account. Such a procedure can be carried out during the base carrying operational traffic and is not limited to offline or even preinstallation calibration. A discussion gives some insights on how to obtain best calibration results.

1 Introduction

According to the error free model, the array receive matrix

$$\mathbf{X} = \mathbf{A} \cdot \mathbf{S} \qquad (1)$$

just depends on the the array steering matrix $\mathbf{A}$ and the signals of the W impinging wavefronts in matrix $\mathbf{S}$. As long as the number of wavefronts W is smaller than the number of antenna elements M the directions can be estimated [3]. Besides additive noise $\mathbf{N}$, mutual coupling and amplification errors represented by matrix $\mathbf{K}$ will cause an accuracy loss if the erroneous receive matrix

$$\tilde{\mathbf{X}} = \mathbf{K} \cdot \mathbf{A} \cdot \mathbf{S} + \mathbf{N} \qquad (2)$$

is used. For this reason calibration schemes like in [8] are essential. Calibration can be achieved by the knowledge of the directions of arrival (DoAs) of wavefronts impinging on an antenna array [7], [1], [5]. In a mobile communication system where the positions of base stations are fixed, this approach is very attractive. Vice versa, smart antennas will provide a considerable capacity gain as already shown in experimental field trials [2].

Figure 1: City map of downtown Munich based on three dimensional building data

The German network operator Mannesmann Mobilfunk GmbH applies raytracing tools for network planning. In this study, these tools are applied to the three dimensional building data (length, width and height) of Munich (cf.Fig.1). Munich has been chosen because the propagation conditions in this city with over one million inhabitants and roof top heights that vary between 10 m and 30 m in a topography which is 500 m to 550 m above sea level can be classified as bad urban.

Fig.2 shows the network configuration of 16 representative base stations surrounding the center base station located in downtown Munich. The DoAs of the wavefronts transmitted by the 16 surrounding base stations as well as their receive powers are evaluated. Fig.3 proves a typical angular spread of the impinging wavefronts besides the LOS (Line of Sight) component received by the center base station. The direction parameters x and y denote the elements of the pointing vector

$$\mathbf{v} = \begin{bmatrix} x \\ y \\ z \end{bmatrix} = - \begin{bmatrix} \cos\epsilon \cdot \cos\alpha \\ \cos\epsilon \cdot \sin\alpha \\ \sin\epsilon \end{bmatrix} , \qquad (3)$$

cf. Fig.4, where the direction of a wavefront impinging on a

0-7803-5599-7/99/$10.00©1999 IEEE

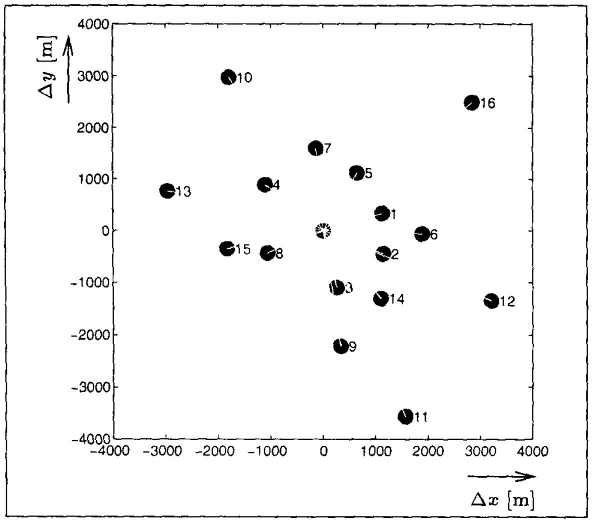

Figure 2: Existing configuration of 16 representative GSM base stations around the base station at (0,0) in the network of Mannesmann Mobilfunk GmbH

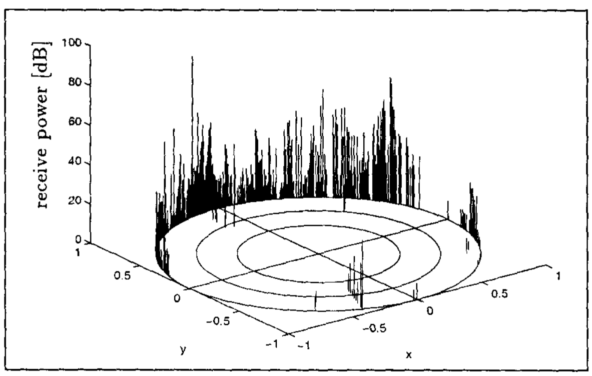

Figure 3: Receive powers and DoAs of wavefronts transmitted by base station 3 and received by the center base station

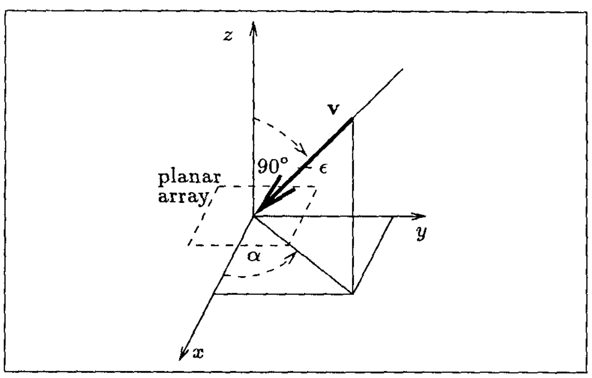

Figure 4: Direction of Arrival (DoA) denoted by azimuth α and elevation ϵ or by vector $\mathbf{v}$

planar array depends on the azimuth α and the elevation ϵ.

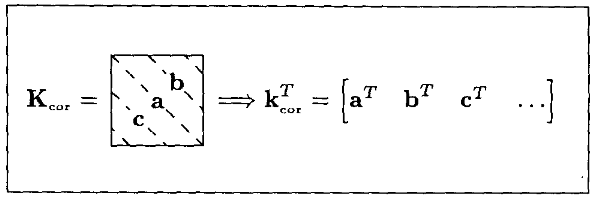

Figure 5: Diagonalwise vectorisation of $\mathbf{K}_{\text{cor}}$

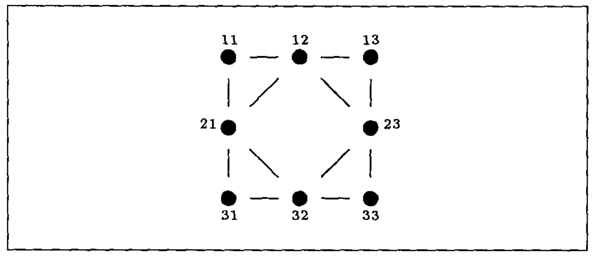

Figure 6: Planar 3×3 frame array

2 Uplink Calibration

In order to obtain the correction matrix $\mathbf{K}_{\text{cor}}$, that perfectly compensates amplification errors and mutual coupling

$$\mathbf{K}_{\text{cor}} \cdot \mathbf{K} = \mathbf{I} \tag{4}$$

in the ideal case, we propose an iterative optimization approach similar to [6] that has been successfully applied to the RUSK radio channel sounder [4]. When matrix $\tilde{\mathbf{M}}_s$ denotes the correlation matrix of the erroneous receive matrix $\tilde{\mathbf{S}}_s$ (2) with respect to the wavefronts transmitted just by base station s and $\hat{\mathbf{K}}^{(l)}_{\text{cor}}$ constitutes the estimated correction matrix at the l-th iteration step, the matrix

$$\hat{\mathbf{M}}_s = \hat{\mathbf{K}}^{(l)^*}_{\text{cor}} \cdot \tilde{\mathbf{M}}_s \cdot \hat{\mathbf{K}}^{(l)^T}_{\text{cor}} \tag{5}$$

leads to a precalibrated array. Similar to spatial smoothing for DoA estimation, the whole antenna array is divided into $M - M_{\text{sub},s} + 1$ subarrays of $M_{\text{sub},s}$ antennas. Again, the index s denotes the affiliation to base station s. Each subarray i owns a weight vector

$$\mathbf{c}_{\text{SP},i,s} = \begin{bmatrix} \mathbf{0}^{i-1\times 1} \\ \mathbf{c}_{i,s}^{M_{\text{sub},s}\times 1} \\ \mathbf{0}^{M-M_{\text{sub},s}+1-i\times 1} \end{bmatrix} \quad . \tag{6}$$

In the case of W_s discrete wavefronts, these weight vectors $\mathbf{c}_{\text{SP},i,s}$ zero all incoming wavefronts as long as $W_s < M_{\text{sub},s}$ is true. In the case of an angular spread for each subarray i and each base station s a vector $\mathbf{c}_{i,s}^{M_{\text{sub},s}\times 1}$ has to be computed that minimizes the receive power

$$p_{\text{rec}} = \mathbf{c}_{i,s}^H \cdot \mathbf{M}_{i,s} \cdot \mathbf{c}_{i,s} \quad . \tag{7}$$

Matrix $\mathbf{M}_{i,s}$ refers to the correlation matrix of the calibrated subarray i and the respective base station s. A diagonalwise vectorization of matrix $\mathbf{K}_{\text{cor}}$ (cf.Fig.5) leads to a vector $\mathbf{k}_{\text{cor}}$ while the elements of vector $\mathbf{c}_{\text{SP,i},s}$ are arranged in a matrix $\mathcal{C}^T(\mathbf{c}_{\text{SP,i},s})$:

$$\mathbf{K}_{\text{cor}}^T \cdot \mathbf{c}_{\text{SP,i},s} = \mathcal{C}^T(\mathbf{c}_{\text{SP,i},s}) \cdot \mathbf{k}_{\text{cor}} \quad . \tag{8}$$

The correlation matrices of the subarrays

$$\bar{\mathbf{M}}_{\text{SP},s}^{\text{UL}} = \sum_{i=1}^{M-M_{\text{sub},s}+1} \mathcal{C}^*(\mathbf{c}_{\text{SP,i},s}) \cdot \hat{\mathbf{M}}_s \cdot \mathcal{C}^T(\mathbf{c}_{\text{SP,i},s}) \tag{9}$$

as well as the correlation matrices of all surrounding S base stations

$$\bar{\mathbf{M}}_{\text{SP}}^{\text{UL}} = \sum_{s=1}^{S} \bar{\mathbf{M}}_{\text{SP},s}^{\text{UL}} \tag{10}$$

are summed up. The eigenvector $\mathbf{k}_{\text{cor}}$ of the corresponding smallest eigenvalue $\lambda_{\min}$ of the generalized eigenvalue problem

$$\bar{\mathbf{M}}_{\text{SP}}^{\text{UL}} \cdot \mathbf{k}_{\text{cor}} - \lambda_{\min} \begin{bmatrix} \mathbf{I}^{M\times M} & \mathbf{0} \\ \mathbf{0} & \mathbf{0} \end{bmatrix} \cdot \mathbf{k}_{\text{cor}} = \mathbf{0} \tag{11}$$

is reshaped towards a matrix

$$\mathbf{K}_{\text{cor}} = \mathcal{K}(\mathbf{k}_{\text{cor}}) \tag{12}$$

according to Fig.5. Finally, updating provides an improved estimation

$$\hat{\mathbf{K}}_{\text{cor}}^{(l+1)} = \mathbf{K}_{\text{cor}} \cdot \hat{\mathbf{K}}_{\text{cor}}^{(l)} \tag{13}$$

of the correction matrix. The performance of this optimization amounts to this: The number of "large" eigenvalues of the correlation matrix $\bar{\mathbf{M}}_{\text{SP}}^{\text{UL}}$ (roughly spoken its rank assuming the "small" eigenvalues are set equal to zero) must not be much smaller than the number of unknown elements in the correction matrix $\mathbf{K}_{\text{cor}}$. The coupling between non-adjacent antenna elements is very small. For that reason it makes sense just to take the coupling between adjacent antenna elements into account. Fig.6 shows the coupling between a planar 3×3 frame array. Its coupling matrix (after lining up the elements in a $11-12-13-21-23-31-32-33$-row)

$$\mathbf{K} = \begin{bmatrix} \bullet & \bullet & & \bullet & & & & \\ \bullet & \bullet & \bullet & \bullet & \bullet & & & \\ & \bullet & \bullet & & \bullet & & & \\ \bullet & \bullet & & \bullet & & \bullet & \bullet & \\ & \bullet & \bullet & & \bullet & & \bullet & \bullet \\ & & & \bullet & & \bullet & \bullet & \\ & & & \bullet & \bullet & \bullet & \bullet & \bullet \\ & & & & \bullet & & \bullet & \bullet \end{bmatrix} \tag{14}$$

has a reduced number of just 32 different and unknown elements marked by abullets. In case of an $M \times M$ frame array, the number of unknown elements is reduced from M^2 to $M + 2 \cdot M + 2 \cdot 4$. For better calibration results, equations (4), (5), and (13) have to be modified with respect to an estimation of $(\hat{\mathbf{K}}_{\text{cor}}^{(l)})^{-1}$ instead of $\hat{\mathbf{K}}_{\text{cor}}^{(l)}$. Besides the total number of S base stations, the number of wavefronts W_s and the subarray size $M_{\text{sub},s}$ play a very important role. Assuming discrete wavefronts, an upper bound of the "rank" of matrix $\bar{\mathbf{M}}_{\text{SP}}^{\text{UL}}$ can be specified. That is

$$r_{\text{coh}} = \sum_{s=1}^{S} (M + 1 - M_{\text{sub},s}) \tag{15}$$

in case of completely coherent wavefronts and

$$r_{\text{unc}} = \sum_{s=1}^{S} W_s \cdot (M + 1 - M_{\text{sub},s}) \tag{16}$$

in case of completely uncorrelated wavefronts (due to a delay exceeding one bit period of GSM).

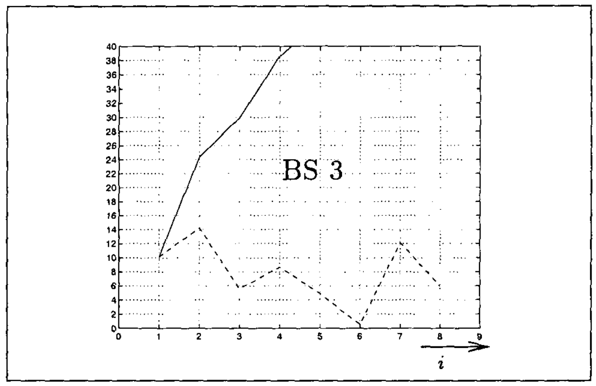

Figure 7: Eigenvalue profile of the correlation matrix $\mathbf{M}_3$. The wavefronts are impinging at a 3×3 antenna array. The solid line denotes $10 \log \frac{\lambda_1}{\lambda_{i+1}}$ and the dotted line $10 \log \frac{\lambda_i}{\lambda_{i+1}}$. The eigenvalues are sorted in descending order.

BS	1	2	3	4	5	6	7	8
20 dB	1	1	2	1	4	1	1	1
30 dB	1	1	3	2	5	3	2	1
40 dB	3	2	4	4	6	3	4	2
BS	9	10	11	12	13	14	15	16
20 dB	1	1	1	1	2	3	2	1
30 dB	3	3	2	1	2	5	3	2
40 dB	5	3	4	2	4	7	5	2

Table 1: Number of effective wavefronts depending on the threshold of 20 dB, 30 dB and 40 dB

Fig.7 presents the eigenvalue profile of a correlation matrix $\mathbf{M}_3$ caused by the wavefronts that are transmitted by base station 3. Depending on the chosen threshold for $10 \log \frac{\lambda_1}{\lambda_{i+1}}$, e.g. 20dB, 30dB, 40dB, the number of wavefronts that have to be taken into account is 2, 3, 4, and the respective subarray size $M_{\text{sub},3}$ equals 3, 4, 5. As for the other base stations, their propagation conditions and effective numbers of wavefronts are similar (cf.Tab.1). An increased subarray size $M_{\text{sub},s}$ diminishes the gain in rank by "spatial smoothing" (9), (15). On the other side the angular spread is better suppressed and according to (16) a gain in rank by uncorrelated wavefronts may be achieved.

3 Simulations

The calibration results support this theoretical view. The Figs. 8 and 9 show the calibration error e_c, that is $\max_i 20\log|e_{ii}|$ with respect to the amplification (solid line) and $\max_{i\neq j} 20\log|e_{ij}|$ with respect to the mutual coupling (dotted line), where e_{ij} denotes an element of

$$\mathbf{E} = \hat{\mathbf{K}}_{\mathrm{cor}}^{(l)}\mathbf{K} - \mathbf{I} \quad . \tag{17}$$

An increased averaging over base station (10) improves the calibration due to (15) and (16). The remaining calibration error e_c in Fig.8 using all of the 16 base stations ($S = 16$) is smaller than the calibration error e_c in Fig.9 using the first four base stations ($S = 4$). A threshold of 40dB (cf.Fig.9) and corresponding subarray sizes (cf.Tab.1) enhance the performance in comparison with a threshold of 20dB (cf.Fig.8). But this is also due to the fact that propagation delay reaches one bit period and wavefronts become uncorrelated. Choosing a subarray size of 3 instead of 2 effects almost a gain in rank by a factor of 2 when 2 uncorrelated wavefronts are impinging (16). With completely correlated wavefronts equation (15) would not provide a sufficient "rank" of matrix $\bar{\mathbf{M}}_{\mathrm{SP}}^{\mathrm{UL}}$.

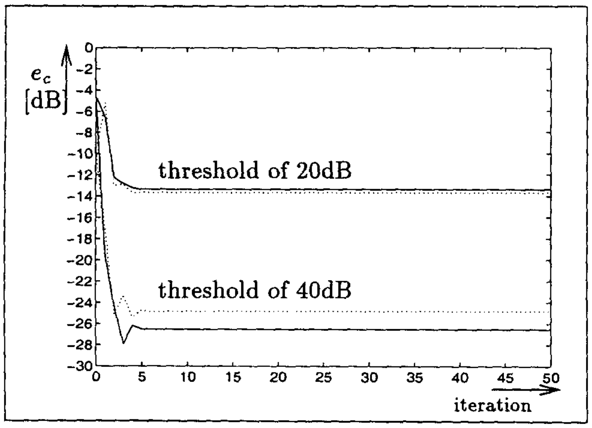

Figure 8: Calibration error e_c versus the iterations. $S = 16$.

4 Conclusions

This study presents the calibration results of general antenna arrays applying the configuration and building data of a real GSM network. For a sufficient suppression of imperfections like mutual coupling and amplification errors the presented direction based calibration has to cope with a considerable angular spread. A properly chosen subarray size that exploits the path delay differences, a model reduced approach with less unknown coupling elements and a suited eigenvalue decomposition achieve the best performance. The calibration can be carried out during operational traffic of the GSM base stations.

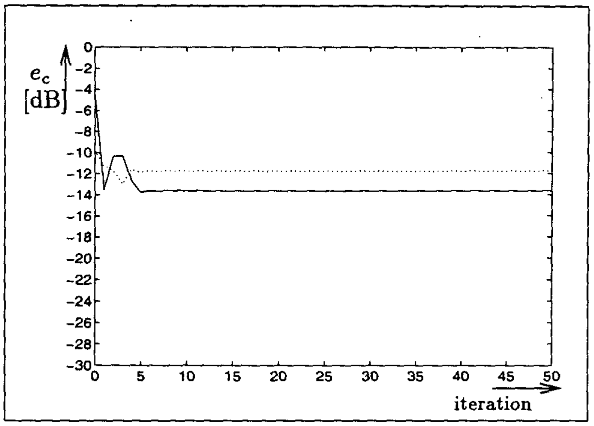

Figure 9: Calibration error e_c versus the iterations. $S = 4$, threshold of 40dB.

References

[1] M. Ali, J. Götze, and R. Pauli. An algorithm for the calibration of sensor arrays with sensor gain and phase uncertainties. *Proceedings IEEE ICASSP*, pages 121–125, Minneapolis, Minnesota, April 1993.

[2] S. Anderson, U. Forssen, J. Karlsson, T. Witzschel, and A. Krug. Ericsson / Mannesmann GSM field-trials with adaptive antennas. *In Proc. European Personal Mobile Communications Conference*, pages 77–85, Bonn, Germany, October 1997.

[3] M. Haardt. Efficient one-, two-, and multidimensional high-resolution array signal processing. *PhD thesis, Technical University of Munich*, 1996.

[4] P.H. Lehne, F. Aanvik, J-C. Bic, P. Pajusco, M. Grigat, I. Gaspard, and U. Martin. Calibration of mobile radio channel sounders. *COST 259 TD (98) 088*, Duisburg, Germany, September 1998.

[5] A. Paulraj and T. Kailath. Direction of arrival estimation by eigenstrucure methods with unknown sensor gain and phase. *ICASSP*, pages 640–643, 1985.

[6] K. Pensel and J.A. Nossek. Uplink and downlink calibration of smart antennas. *In Proc. Int. Conf. on Telecomm. (ICT 98)*, Porto Carras, Greece, 22-25 June 1998.

[7] J. Pierre and M. Kaveh. Experimental performance of calibration and direction-finding algorithms. *ICASSP*, pages 1365–1368, 1991.

[8] Y. Rockah and P.M. Schultheiss. Array shape calibration using sources in unknown locations - part i. *IEEE Trans. on ASSP*, 35(3):286–299, March 1987.